

## Metal–Metal Interactions

DOI: 10.1002/ange.200600800

## Conductance and Stochastic Switching of Ligand-Supported Linear Chains of Metal Atoms\*\*

I-Wen Peter Chen, Ming-Dung Fu, Wei-Hsiang Tseng,  
Jian-Yuan Yu, Sung-Hsun Wu, Chia-Jui Ku,  
Chun-hsien Chen,\* and Shie-Ming Peng\*

Molecular wires and switches are forecast to be the elemental building blocks for future electronic applications. Synthesiz-

[\*] I.-W. P. Chen, M.-D. Fu, W.-H. Tseng, J.-Y. Yu, S.-H. Wu, C.-J. Ku, Prof. C.-h. Chen<sup>[†]</sup>  
Department of Chemistry  
National Tsing Hua University  
Hsinchu, Taiwan 30013 (Republic of China)  
Fax: (+886) 3-571-1082  
E-mail: chhchen@mx.nthu.edu.tw

Prof. S.-M. Peng  
Department of Chemistry  
National Taiwan University  
Taipei, Taiwan 106 (Republic of China)  
and  
Institute of Chemistry  
Academia Sinica  
Taipei, Taiwan 115 (Republic of China)  
Fax: (+886) 2-2363-6359  
E-mail: smpeng@ntu.edu.tw

[†] Current Address:  
Department of Chemistry  
National Taiwan University  
Taipei, Taiwan 106 (Republic of China)  
Fax: (+886) 2-2363-6359

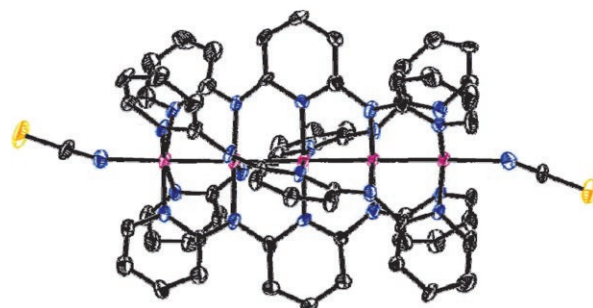
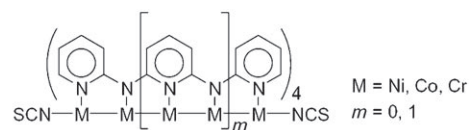
[\*\*] Thanks to Professor I.-C. Chen (NTHU) for fruitful discussions, to Dr. Andy H. Kung (IAMS, Academia Sinica, Taipei) for comments on the manuscript and to collaborators of S.-M.P. for the routine supply of metal string complexes. C.-h.C. acknowledges Professor T.-Y. Luh (NTU) for use of a NanoScope IIIa and the Department of Chemistry (NTHU) for the strong research support. This work was funded by the National Science Council and the Ministry of Education of the Republic of China.



Supporting information for this article is available on the WWW under <http://www.angewandte.org> or from the author.

ing 1D molecules and comprehensively understanding their electric characteristics has become one of the major focus areas of materials science. The growth of this research field has been encouraged by the discovery of a strong dependence of electron transport on the length, conjugation, conformation, and substituents of tailored molecules.<sup>[1,2]</sup> While remarkable progress has been achieved during the past decade, most of the knowledge learned has been from conjugated organic molecules whose counterpart, organometallic molecular wires,<sup>[3–17]</sup> has been rarely explored.

Herein we present quantitative measurements of single-molecule conductance of 1D multinuclear metal strings ( $[M_n L_4(NCS)_2]$ ,  $M_n = Cr_3, Co_3, Ni_3, Cr_5, Co_5, Ni_5$ , and  $Cr_7$ ;  $L = \text{oligo-}\alpha\text{-pyridylamine}$ ; Scheme 1).<sup>[3]</sup> The conductance



**Scheme 1.** Top: The metal atom chain is supported by four oligo- $\alpha$ -pyridylamine ligands.<sup>[3]</sup> Bottom: ORTEP view of the pentacobalt complex;<sup>[19]</sup> in general the metal atoms are collinear and wrapped helically by four ligands. Co purple, N blue, S yellow, C gray.

values correlate well with the d-orbital electronic coupling between adjoining metal atoms. Among the strings, penta- and heptachromium complexes exhibit stochastic switching events. Such multinuclear strings are important in setting up a perfect platform for the study of metal–metal interactions beyond dinuclear complexes.<sup>[18]</sup> Complexes up to nonanickel (i.e.,  $M = Ni$ ,  $m = 3$  in Scheme 1, but with Cl axial ligands) have been characterized crystallographically<sup>[3]</sup> and the length of the ligand extended up to 12 repetitive pyridylamine units ( $m = 11$ ). While purification and crystallization become increasingly challenging owing to poorer solubility for longer oligomers, preliminary MALDI-MS spectra show that a string of 17 nickel ions ( $m = 7$  in Scheme 1) is obtainable. An understanding of the conduction propagating along the metal chains will further advance progress towards molecular wires for nanodevices.

Figure 1 shows the results of STM (scanning tunneling microscopy) break junction for the trinuclear and pentanuclear string complexes.<sup>[20,21]</sup> Experimental procedures were documented in detail by the groups of Tao and Lindsay.<sup>[20,21]</sup>

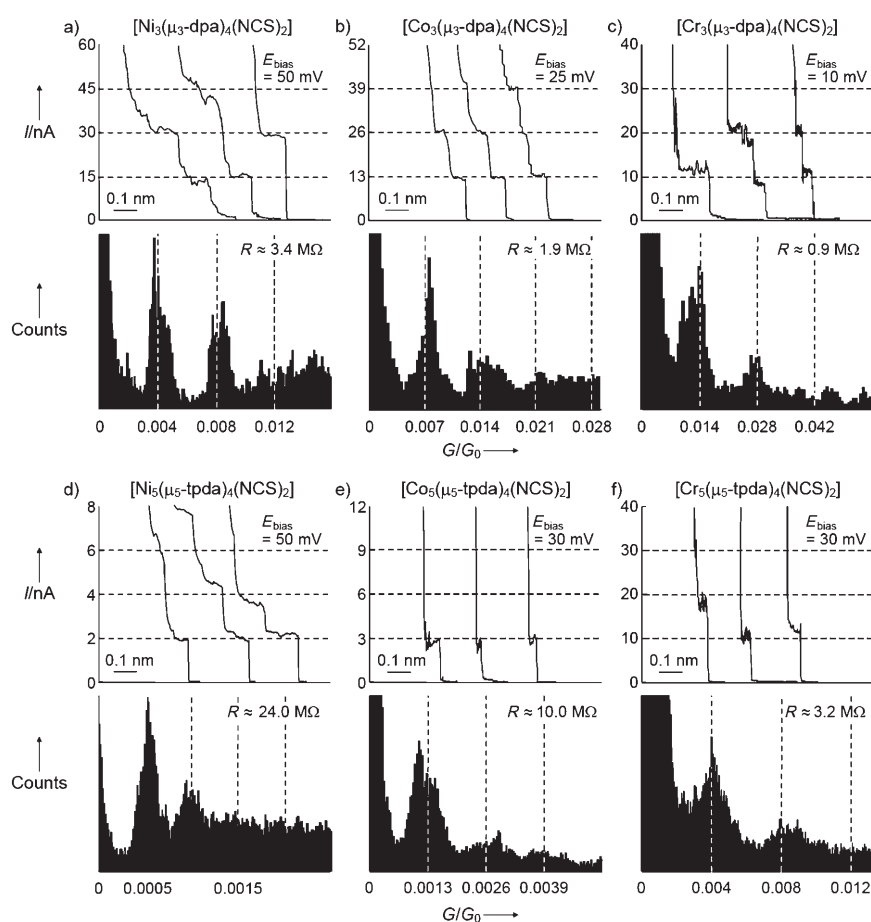


**Figure 1.** a)–f) Single-molecule conductance of metal strings measured by STM break junction. Top panels: typical current curves acquired by stretching the molecular junctions are presented with arbitrary x-axis offsets. Currents and conductance of the metal string complexes decrease in quantized steps. Bottom panels: the conductance histograms are obtained from more than 2000 measurements. The resistance of a single heptachromium string is 6.9 M $\Omega$  (see Supporting Information). In the absence of molecules, no such steps or peaks are observed within the same conductance range.

Briefly, housed in a nitrogen-filled chamber, a gold STM tip is brought into and out of contact with a gold substrate in toluene, which also contains the metal strings. Upon repeated formation of the tip–substrate gap, the isothiocyanate axial ligands at the termini of the metal strings bind to the gold electrodes and complete a molecular junction. At a fixed bias voltage across the electrodes ( $E_{bias}$ , top panels of Figure 1), the STM tip is pulled away from the substrate, which results in the currents monitored having a stepped profile. The current values are scaled with  $E_{bias}$ . Controlled experiments in toluene gave exponential tunneling decay,<sup>[20,21]</sup> thus confirming that the “staircase” waveforms arise from the metal strings.

The histograms (bottom panels of Figure 1) plotted against  $G/G_0$  ( $G_0$  = conductance quantum for the cross section of a metallic contact being only that of a single atom;  $G_0 = 2e^2/h$ ,  $\approx (12.9$  k $\Omega)^{-1}$ ).<sup>[20–23]</sup> summarize thousands of measurements. The local maxima are distributed at integer multiples of the fundamental  $G_0$  values of each molecule, which suggests that the number of molecules in the junctions is one, two, three, etc.<sup>[20,21]</sup> The top-right corner of each

histogram states the single-molecular resistance,  $R$ , which is calculated by dividing  $E_{bias}$  by the fundamental current.

Although the conjugated oligopyridylamido ligand and tunneling events along the metal chains might be involved in the conduction mechanism, given that each chain has identical ligands, analogous crystallographic structures, and similar physical dimensions,<sup>[3,19,24–29]</sup> the discrepancy between the molecular resistances of the chains most likely lies in the extent of coupling of the d-orbital electrons between adjoining metal atoms. In ascending order of conductance the sequence is nickel, cobalt, and chromium for strings with the same number of metal centers. This trend correlates well with the results of extended Hückel (EH) MO calculations in which the d-electron configurations for pentanickel,<sup>[25]</sup> pentacobalt,<sup>[25]</sup> and pentachromium<sup>[26]</sup> strings are  $\sigma_1^2\pi_1^4\sigma_2^2\pi_2^4\delta_{n1}^2\delta_{n2}^2\pi_{n3}^4\delta_{n3}^2\pi_{n4}^4\delta_{n4}^2\pi_{n5}^4\delta_{n5}^2\sigma_{n3}^2\sigma_{n4}^2\sigma_{n5}^2$ ,  $\sigma_1^2\pi_1^4\sigma_2^2\pi_2^4\delta_{n1}^2\delta_{n2}^2\pi_{n3}^4\delta_{n3}^2\pi_{n4}^4\delta_{n4}^2\pi_{n5}^4\delta_{n5}^2\sigma_{n3}^1$ , and  $\sigma_1^2\sigma_2^2\pi_1^4\pi_2^4\delta_{n1}^2\delta_{n2}^2\delta_{n3}^2\pi_{n(dxy)}^1\pi_{n(dyz)}^1$ , respectively (where the subscript  $n$  denotes non-bonding). The metal–metal bond orders for strings of nickel, cobalt, and chromium cores are 0, 0.5, and 1.5, respectively; these values indicate the degree of electron delocalization and thus the efficiency of electrons conducting through the metal centers.

The resistance of single molecules is also described by a tunneling decay constant,  $\beta$ , approximately given by  $I \propto \exp(-\beta x)$ , in which  $x$  is either the number of repetitive units or the molecular dimensions and  $I$  is the current.  $\beta$  represents the electronic-coupling strength of the molecule along the electron pathway. A small  $\beta$  value indicates a less significant impedance in electron transport through the molecule. By taking the natural logarithm of the reciprocal of resistance values against the molecular length, we obtain a small tunneling decay constant of 0.50 per Cr atom or approximately 0.21 Å<sup>−1</sup> (see Supporting Information), which makes the Cr strings among the most conductive molecular wires reported.<sup>[2,30]</sup>

In addition to their extraordinary conductive properties, the metal strings of penta- and heptachromium complexes show an electric switching phenomenon that is not readily discernible by STM break junction. The on/off states of the two chromium strings are revealed by the conductive atomic force microscopy (CAFM) developed by Lindsay and co-workers.<sup>[31]</sup> The metal strings are attached to a gold surface and isolated within an *n*-alkanethiol matrix. The films are then incubated for 1–3 h in dichloromethane containing

triphenylphosphine-stabilized gold clusters (nominally 2 nm in diameter).<sup>[31,32]</sup> A metal–molecule–nanocluster junction is configured through the isothiocyanate axial ligands. The gold clusters improve the electrical contact with the gold-coated cantilever of the CAFM and enable highly reproducible current-versus-potential ( $I$ – $V$ ) measurements for single molecules.<sup>[31,32]</sup> Figure 2a demonstrates that more than 2500  $I$ – $V$

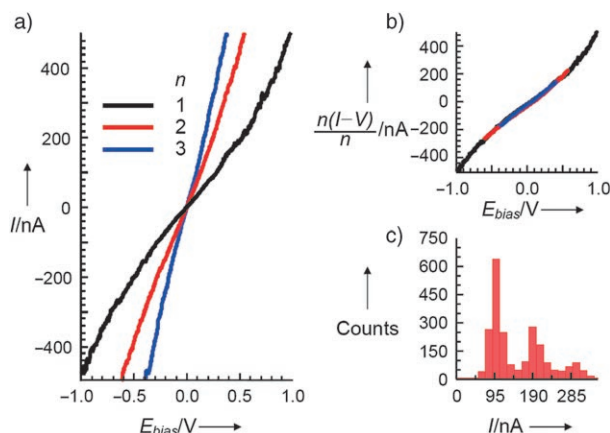


**Figure 2.**  $I$ – $V$  data of  $[Cr_3(\mu_3\text{-dpa})_4(\text{NCS})_2]$  in an  $n$ -octanethiol matrix measured by CAFM, see text for details. a)  $I$ – $V$  curves of groups centered at integral multiples  $n$  of a single-molecule conductance. b) Overlap of the curves in (a) after being divided by  $n$  at each point. c) Histogram plot of the currents measured at 0.25 V bias. The CAFM experiments were carried out in toluene under nitrogen. The force was constantly monitored and set at 2.5 nN.

measurements of the trichromium complex can be grouped into three curves, which converge into one after the values of the curves are divided by  $n$  (Figure 2b;  $n=2$  and 3, for the red and blue curves, respectively). Figure 2c is a histogram of the currents measured at a bias of 0.25 V. The strong correlation of an integral multiplicity between the three groups suggests that the one centered at 95 nA corresponds to the primary case of a single trichromium metal string sandwiched between a gold nanocluster and the substrate.

The  $I$ – $V$  curves and histograms for all the metal strings show a similar quantized behavior, which is consistent with the findings revealed by STM break junction, although this CAFM approach is complicated by Coulomb blockade charged at the attached gold cluster and thus the essence of the  $I$ – $V$  curves is not straightforward.<sup>[32]</sup> The fundamental curves of the single trinuclear and pentanuclear strings are summarized in Figures 3a and b. Note that the pentachromium string shows two fundamental curves with current values of about 410 and 66 nA at a bias of 1.0 V (blue curves in Figure 3b). The heptachromium string complex also has two sets of  $I$ – $V$  curves with 252 and 56 nA at a bias of 1.0 V (see Supporting Information).

Readily discernible from their histograms at a bias of 0.25 V are two sets of fundamental current values centered at 74 and 17 nA (Figure 3c) for the pentachromium string, and at 50 and 10 nA (Figure 3d) for the heptachromium string. The dataset of the more conductive complex has a  $\beta$  value of 0.16 per Cr atom, thus indicating a stronger electronic

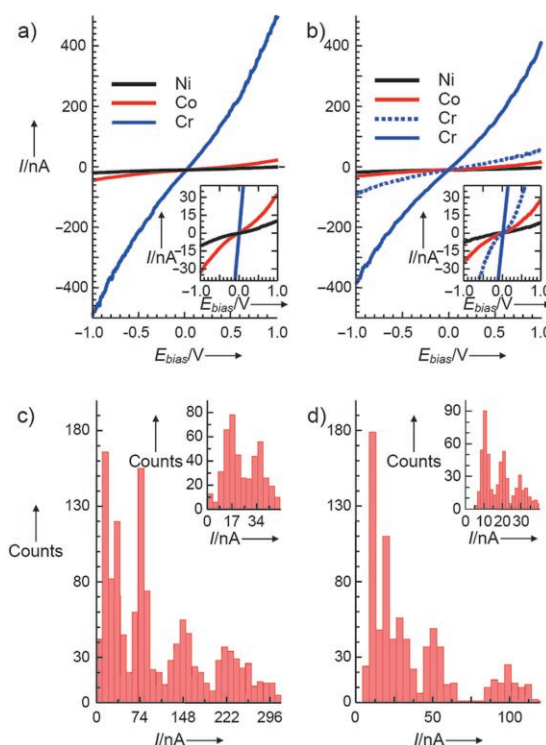


**Figure 3.**  $I$ – $V$  characteristics of metal strings measured by CAFM. Fundamental  $I$ – $V$  curves of a) the trinuclear and b) the pentanuclear complexes and magnified view of the traces between  $\pm 40$  nA (insets). Histograms of the currents measured at a bias of 0.25 V for c) the pentachromium and d) the heptachromium complexes; insets show the same histograms plotted with a narrower bin size (that is, the width of the histogram bars is smaller) to magnify the current range for the less conductive groups. Tri-, penta-, and heptanuclear complexes were isolated in matrices of  $n$ -octanethiol,  $n$ -tetradecanethiol, and  $n$ -octadecanethiol monolayers, respectively.

coupling than the  $\beta$  value of 0.29 per Cr atom derived from dataset of the less conductive complex. Although the  $\beta$  values are not quantitative owing to Coulomb blockade,<sup>[32]</sup> the substantial difference between the two values suggests that the two sets of conductance peaks are not due to the S–Au contacts at atop and hollow sites.<sup>[21]</sup> The ratio of the occurrence of the smaller-current dataset to that of the larger-current dataset is 345:1251 and 970:200 for penta- and heptachromium strings, respectively. The fraction of the smaller-current dataset increases with the number of chromium cores. Note that the trichromium metal string does not show two sets of primary  $I$ – $V$  curves, which suggests that the less-conductive set is either absent or very rare.

The imaging frames of conducting-current mode in Figure 4 display the electric switching of the pentachromium molecule. Figure 4a shows the current toggling between a low value of 17 nA and a high value of about 75 nA. In Figures 4b and c, the current switches between twice that of the less conductive mode and twice that of the more conductive mode, which suggests the presence of two pentachromium strings underneath the gold nanocluster (Figure 4d). Stochastic on/off switching has been observed in  $\pi$ -electron conjugated systems and alkanethiols. Recent findings narrow down the switching mechanisms to conformation effects<sup>[33]</sup> on through-

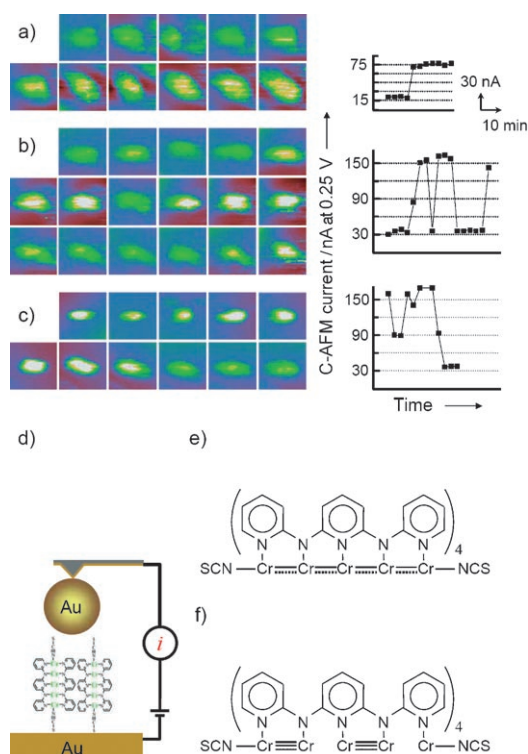


**Figure 4.** Electric on/off switching of pentachromium strings within an *n*-tetradecanethiol matrix. a)–c) Sequential images and the plots of conducting current versus time were acquired by CAFM at a bias of 0.25 V. The time interval between each frame (30 × 30 nm) was about 3 min. The corresponding current magnitudes indicate that underneath each gold nanocluster ( $\approx 2$  nm in diameter) there is one molecule for (a) and two molecules for (b) and (c). d) Circuit diagram of the apparatus used to take the CAFM measurements showing two string molecules under the gold nanocluster. e), f) Structures of the pentachromium metal string with delocalized (on state) and alternating (off state) Cr–Cr bonds, respectively.

bond or through-space tunneling<sup>[34]</sup> and to sulfur–substrate fluctuations through bond breaking or molecular tilt angles associated with the  $sp$  or  $sp^3$  hybridization of the sulfur atom.<sup>[35–37]</sup>

For the molecular wires studied herein, the stochastic switching cannot be entirely explained by sulfur–substrate fluctuations because all the complexes have the same axial ligand, isothiocyanate, yet only penta- and heptachromium strings clearly exhibit two sets of fundamental curves. In addition, the difference in  $\beta$  values and the strong correlation of the number of chromium cores with the occurrence frequency suggest a significant effect of metal–metal interactions on the molecular conductance. The aforementioned EHMO calculations were based on delocalized conformations (or symmetric metal–metal bond lengths) and are unequivocal for nickel<sup>[4,25]</sup> and cobalt<sup>[4,19,27]</sup> strings with isothiocyanate axial ligands. For chromium strings, treatment to refine crystallographically disordered chromium centers found alternative bond lengths with a difference ( $\Delta d_{Cr-Cr}$ ) of 0.25 Å and 0.65 Å for tri-<sup>[28]</sup> and pentachromium<sup>[29]</sup> strings, respectively.

The crystal structures of trichromium strings are sensitive to subtle factors such as solvent and temperature during crystallization, and to different axial ligands.<sup>[24,28,29]</sup> Density functional theory (DFT) calculations of a trichromium analogue,  $[Cr_3(dpa)_4Cl_2]$ , by Rohmer and Benard gave a symmetric (i.e., delocalized) structure at the shallow ground state and a conformation with alternating bond lengths at slightly higher states.<sup>[24,28]</sup> The calculated energies relative to the symmetric conformation are 0.97 kcal mol<sup>−1</sup> and 4.25 kcal mol<sup>−1</sup> for a slightly unsymmetrical ( $\Delta d_{Cr-Cr} = 0.106$  Å) and a localized state ( $\Delta d_{Cr-Cr} = 0.679$  Å), respectively. Thus, it is possible that penta- and heptachromium strings with delocalized and alternating Cr–Cr bonds are present simultaneously and that these delocalized and alternating states are interchangeable in the *n*-alkanethiol matrix (Figures 4e and f). However, as there is an energy difference of less than 5 kcal mol<sup>−1</sup> between the delocalized and localized states of the trichromium complex, the switching rate observed for the pentachromium string is slow. Theoretical studies and variable-temperature experiments will be carried out to elicit the activation energy and switching mechanism.

We have demonstrated that conductance in metal string complexes correlates well with the metal–metal bond order. Penta- and heptachromium strings each exhibit two sets of primary *I*–*V* curves, ascribed to conformations of delocalized and alternating Cr–Cr bond lengths; electrons in the latter are localized, which results in a molecular conductance inferior to that of the delocalized conformation. The molecules are stable under ambient conditions and can offer stringent tests of our understanding of interatomic interactions.

Received: March 1, 2006

Revised: May 5, 2006

Published online: July 27, 2006

**Keywords:** electron transport · metal–metal interactions · molecular electronics · scanning probe microscopy · single-molecule studies

- [1] *Molecular Nanoelectronics* (Eds.: M. A. Reed, T. Lee), American Scientific Publishers, Stevenson Ranch, CA, **2003**.
- [2] D. M. Adams, L. Brus, C. E. D. Chidsey, S. Creager, C. Creutz, C. R. Kagan, P. V. Kamat, M. Lieberman, S. Lindsay, R. A. Marcus, R. M. Metzger, M. E. Michel-Beyerle, J. R. Miller, M. D. Newton, D. R. Rolison, O. Sankey, K. S. Schanze, J. Yardley, X. Zhu, *J. Phys. Chem. B* **2003**, *107*, 6668–6697.
- [3] C.-Y. Yeh, C.-C. Wang, C.-h. Chen, S.-M. Peng in *Nano Redox Sites: Nano-Space Control and its Applications* (Ed.: T. Hirao), Springer, Berlin, **2006**, chap. 5, pp. 85–117.
- [4] S.-Y. Lin, I.-W. P. Chen, C.-h. Chen, M.-H. Hsieh, C.-Y. Yeh, T.-W. Lin, Y.-H. Chen, S.-M. Peng, *J. Phys. Chem. B* **2004**, *108*, 959–964.
- [5] P. Braunstein, C. Frison, N. Oberbeckmann-Winter, X. Morise, A. Messaoudi, M. Benard, M.-M. Rohmer, R. Welter, *Angew. Chem.* **2004**, *116*, 6246–6251; *Angew. Chem. Int. Ed.* **2004**, *43*, 6120–6125.
- [6] E. Goto, R. A. Begum, S. Zhan, T. Tanase, K. Tanigaki, K. Sakai, *Angew. Chem.* **2004**, *116*, 5139–5142; *Angew. Chem. Int. Ed.* **2004**, *43*, 5029–5032.
- [7] J. F. Berry, F. A. Cotton, C. A. Murillo, *Organometallics* **2004**, *23*, 2503–2506.



- [8] A. S. Blum, T. Ren, D. A. Parish, S. A. Trammell, M. H. Moore, J. G. Kushmerick, G.-L. Xu, J. R. Deschamps, S. K. Pollack, R. Shashidhar, *J. Am. Chem. Soc.* **2005**, *127*, 10010–10011.
- [9] G.-L. Xu, R. J. Crutchley, M. C. DeRosa, Q.-J. Pan, H.-X. Zhang, X. Wang, T. Ren, *J. Am. Chem. Soc.* **2005**, *127*, 13354–13363.
- [10] J. Park, A. N. Pasupathy, J. I. Goldsmith, C. Chang, Y. Yaish, J. R. Petta, M. Rinkoski, J. P. Sethna, H. D. Abruña, P. L. McEuen, D. C. Ralph, *Nature* **2002**, *417*, 722–725.
- [11] C. Tejel, M. A. Ciriano, B. E. Villarroja, J. A. Lopez, F. J. Lahoz, L. A. Oro, *Angew. Chem.* **2003**, *115*, 547–550; *Angew. Chem. Int. Ed.* **2003**, *42*, 529–532.
- [12] W. Liang, M. P. Shores, M. Bockrath, J. R. Long, H. Park, *Nature* **2002**, *417*, 725–729.
- [13] X. Lu, K. W. Hipps, X. D. Wang, U. Mazur, *J. Am. Chem. Soc.* **1996**, *118*, 7197–7202.
- [14] T. L. Schull, J. G. Kushmerick, C. H. Patterson, C. George, M. H. Moore, S. K. Pollack, R. Shashidhar, *J. Am. Chem. Soc.* **2003**, *125*, 3202–3203.
- [15] J. G. Kushmerick, D. B. Holt, S. K. Pollack, M. A. Ratner, J. C. Yang, T. L. Schull, J. Naciri, M. H. Moore, R. Shashidhar, *J. Am. Chem. Soc.* **2002**, *124*, 10654–10655.
- [16] J. K. Bera, K. R. Dunbar, *Angew. Chem.* **2002**, *114*, 4633–4637; *Angew. Chem. Int. Ed.* **2002**, *41*, 4453–4457, and references therein.
- [17] H. Vahrenkamp, A. Geiß, G. N. Richardson, *J. Chem. Soc. Dalton Trans.* **1997**, 3643–3651.
- [18] F. A. Cotton, R. A. Walton, *Multiple Bonds between Metal Atoms*, Oxford University Press, New York, **1993**.
- [19] S.-J. Shieh, C.-C. Chou, G.-H. Lee, C.-C. Wang, S.-M. Peng, *Angew. Chem.* **1997**, *109*, 57–59; *Angew. Chem. Int. Ed. Engl.* **1997**, *36*, 56–59.
- [20] B. Xu, N. J. Tao, *Science* **2003**, *301*, 1221–1223.
- [21] X. Li, J. He, J. Hihath, B. Xu, S. M. Lindsay, N. J. Tao, *J. Am. Chem. Soc.* **2006**, *128*, 2135–2141.
- [22] H. Ohnishi, Y. Kondo, K. Takayanagi, *Nature* **1998**, *395*, 780–783.
- [23] A. I. Yanson, G. Rubio-Bollinger, H. E. van den Brom, N. Agrait, J. M. van Ruitenbeek, *Nature* **1998**, *395*, 783–785.
- [24] M.-M. Rohmer, M. Benard, *J. Cluster Sci.* **2002**, *13*, 333–353, and references therein.
- [25] C.-C. Wang, W.-C. Lo, C.-C. Chou, G.-H. Lee, J.-M. Chen, S.-M. Peng, *Inorg. Chem.* **1998**, *37*, 4059–4065.
- [26] H.-C. Chang, J.-T. Li, C.-C. Wang, T.-W. Lin, H.-C. Lee, G.-H. Lee, S.-M. Peng, *Eur. J. Inorg. Chem.* **1999**, 1243–1251.
- [27] R. Clerac, F. A. Cotton, S. P. Jeffery, C. A. Murillo, X. Wang, *Inorg. Chem.* **2001**, *40*, 1265–1270.
- [28] J. F. Berry, F. A. Cotton, T. Lu, C. A. Murillo, B. K. Roberts, X. Wang, *J. Am. Chem. Soc.* **2004**, *126*, 7082–7096, and references therein.
- [29] J. F. Berry, F. A. Cotton, C. S. Fewox, T. Lu, C. A. Murillo, X. Wang, *Dalton Trans.* **2004**, 2297–2302.
- [30] K. Moth-Poulsen, L. Patrone, N. Stühr-Hansen, J. B. Christensen, J.-P. Bourgoin, T. Bjørnholm, *Nano Lett.* **2005**, *5*, 783–785.
- [31] X. D. Cui, A. Primak, X. Zarate, J. Tomfohr, O. F. Sankey, A. L. Moore, T. A. Moore, D. Gust, G. Harris, S. M. Lindsay, *Science* **2001**, *294*, 571–574.
- [32] J. Tomfohr, G. Ramachandran, O. F. Sankey, S. M. Lindsay in *Introducing Molecular Electronics*, Vol. 680 (Eds.: G. Cuniberti, G. Fagas, K. Richter), Springer, Berlin, **2005**, pp. 301–312.
- [33] R. Ochs, D. Secker, M. Elbing, M. Mayor, H. B. Weber, *Faraday Discuss.* **2006**, *131*, 281–289.
- [34] W. Haiss, H. van Zalinge, D. Bethell, J. Ulstrup, D. J. Schiffrin, R. J. Nichols, *Faraday Discuss.* **2006**, *131*, 253–264.
- [35] G. K. Ramachandran, T. J. Hopson, A. M. Rawlett, L. A. Nagahara, A. Primak, S. M. Lindsay, *Science* **2003**, *300*, 1413–1416.
- [36] A. M. Moore, A. A. Dameron, B. A. Mantooth, R. K. Smith, D. J. Fuchs, J. W. Cizek, F. Maya, Y. Yao, J. M. Tour, P. S. Weiss, *J. Am. Chem. Soc.* **2006**, *128*, 1959–1967.
- [37] H. Basch, R. Cohen, M. A. Ratner, *Nano Lett.* **2005**, *5*, 1668–1675.